

Study of Quality Factor and Hysteresis Associated with the State-of-the-art Passive Seismic Isolation System for Gravitational Wave Interferometric Detectors

R. Desalvo^{a*}, Sz. Márka^a, K. Numata^{b, c}, V. Sannibale^a, A. Takamori^{a, d}, H. Tariq^{a*},
E.J. Ugas^a, T. Yoda^a, Y. Aso^a, A. Bertolini^e

^aLIGO laboratory, California Institute of Technology, 1200 E. California Blvd., Pasadena, CA 91125, (USA)

^bDepartment of Physics, University of Tokyo, 7-3-1 Hongo, Bunkyo-ku, Tokyo 113-0033, (Japan)

^cNow at NASA Goddard Space Flight Center, Greenbelt, MD 20771, (USA)

^dNow at Division of Monitoring & Computational Geoscience, Earthquake Research Institute, University of Tokyo, 1-1-1 Yayoi, Bunkyo-ku, Tokyo 113-0032, (Japan)

^eUniversita di Pisa, Dipartimento di Fisica and INFN, Via Buonarroti, 2, 56127 Pisa, (Italy)

LIGO publication number: P-040002-00-D

Keywords: Gravitational waves, Seismic Isolation, Cantilever springs, Maraging, Creep.

PACS

04.80.Nn Gravitational wave detectors and experiments

04.80.Cc Experimental tests of gravitational theories

Abstract

Seismic isolation systems, consistent of passive attenuators, based on mechanical harmonic oscillators with resonant frequencies below the frequency region of interest, are being used by multiple Gravitational wave (GW) detectors. We conduct a study of the fundamental limitations present due to the properties of the material such as Maraging steel, used in some of the seismic attenuation systems for GW detectors. We tentatively interpret the main effects observed in our system, such as the anomalous damping and the hysteresis, in terms of movement of dislocations trapped between Maraging steel intermetallic precipitates. In light of our understanding we further discuss and propose ideas to overcome these limitations and improve the performance of these systems, which may allow for passive attenuation at even lower frequency regimes than achieved so far. These advanced performances would help further reduce the requirements on the mirror suspension control actuators and could reduce their associated noise in the present GWID. This advancement can lead to more suitable seismic attenuation systems for the future instruments with lower frequency sensitivity requirements.

* Corresponding authors: Hareem Tariq htariq@caltech.edu and Riccardo DeSalvo, Tel.: 626 395 2968; fax: 626 395 3814; riccardo@caltech.edu

Introduction

Some of the best performing seismic attenuation systems for Gravitational Wave Interferometric Detectors (GWID) are passive attenuators based on harmonic oscillators with resonant frequencies below the frequency region of interest. These consist of Inverted Pendula (IP) and normal pendula for isolation in the horizontal direction, and soft springs for the vertical direction. The most common vertical springs are cantilever blades softened by different anti-spring configurations, magnetic in Virgo [1, 2, 3], geometric in the Advanced LIGO [4] and TAMA [5, 6, 7] suspension prototypes. GEO [8] and Advanced LIGO use Virgo like blades, without anti-springs, due to the less stringent low frequency seismic attenuation requirements specified for those interferometers [9, 10]. The cantilever springs in the TAMA-SAS prototype are equipped with the most advanced version of anti-springs, the Monolithic Geometric Anti Spring (MGAS) [11, 12]. Other configurations like Lacrosse and Euler springs were used in prototypes for ACIGA [13].

While tuning the MGAS filter and the IP developed for the Advanced LIGO seismic attenuation prototype towards lower frequencies, we observed a progressive decrease in their Quality factors. Typically, the oscillator's Q-factor approached unity below 20 mHz for IP and below 200 to 500 mHz for MGAS filters, depending on the dimensions and the material used for construction. Smaller sized MGAS approach unitary Q-factors at higher frequencies.

The Q-factor approaches unity as the oscillation frequency is tuned down. It is observed that eventually the restoring forces become so weak that static frictional forces appear and start to dominate. At sufficiently low resonant frequencies, the oscillator reaches metastable equilibrium positions within a frequency region around the equilibrium point, which can grow as the oscillator is tuned to lower frequencies.

The decrease in Q-factor can be explained by the fact that, while the amount of elastic energy exchanged per cycle remains roughly constant, the oscillation kinetic energy decreases as the square of the frequency. The resulting Q-factor (the ratio of the oscillation kinetic energy over the losses) then should decrease accordingly and that is, qualitatively, what our measurements show.

At these critical tuning conditions, the hysteresis produced an apparently unpredictable behavior under the influence of large external excitations, which include load changes

and large seismic excitations (e.g. earthquakes). Some of these effects were already observed in the Virgo magnetic anti-springs [14], earlier MGAS filters [15] and IP.

The Q-factor approaches unity and hysteresis becomes significant at frequencies ten times higher in the MGAS springs than in the IP. A possible explanation for this frequency shift will be explained below.

It is important to note that, contrary to what is stated in [1], a high mechanical Q-factor is not a necessary condition for the best performance of a seismic attenuation system. Actually a decreased Q factor has a beneficial effect both on IP and MGAS filters because sufficiently low Q factors eliminate the need of resonance damping (inertial, Eddy or active) of the system. It is true that viscous friction introduces a $1/v$, where v is the frequency, component that adds to the $1/v^2$ transfer function behavior of a pure (lossless) harmonic oscillator, but in virtually all cases the $1/v$ component has such a small coefficient that it becomes relevant only at frequencies above the GWID frequency region of interest and has no practical influence on the overall attenuation system's transfer function. Also the observed damping is more compatible with internal friction (losses proportional to integrated displacement) than viscous damping (losses proportional to speed). The dissipation in the springs can though contribute to the thermal noise performance of the mirror suspensions at the lowest stages of a seismic attenuation system. It can be easily calculated that the low frequency tuning with anti springs does not in itself modify the spring's dissipation effects that may percolate to the mirror suspension thermal noise and affect its performance. Therefore if the intrinsic loss mechanisms are not modified then the anti springs only affect the attenuation transfer function shape and the lowest portion of the suspension thermal noise without affecting the high frequency part [16]. Springs with high Q-factors are still required close to the mirrors whether they are equipped with anti-springs or not.

The hysteresis of springs can be problematic if it causes significant drifts of the equilibrium point. It was observed that hysteresis simply displaced the oscillator's equilibrium point as a result of large excursions and then, for small oscillations, the oscillator worked stably and regularly. The main problem is that, at sufficiently low frequencies, onset of critical damping makes it impossible to let the springs oscillate sufficiently to determine and tune their effective oscillation frequency and working point. The presence of these less understood frictional forces (critical behavior and random offset of the equilibrium point) initially prevented the tuning of the MGAS oscillators (and even the IPs) to lower resonant frequencies. Practical techniques to overcome the difficulties of setting the working point introduced by the hysteresis, and of frequency tuning when the springs are critically damped, as well as methods to control thermal sensitivity enhanced by the low frequency tuning, are further studied by the authors [17]. Since all specifications for GWID isolation system were met by MGAS and IPs [18, 19], neither critical damping nor hysteresis were ever a concern for our system, therefore these issues were not studied or addressed before this paper.

We tentatively interpret both effects, critical behavior and hysteresis, in terms of dislocations trapped between Maraging steel intermetallic precipitates, but otherwise mostly free to move. These dislocations may slosh back and forth under the oscillating stress field, thus giving rise to a dissipation mechanism. A small number of these

dislocations can get temporarily tangled with the precipitates, and can then provide the memory necessary to generate the reversible hysteresis observed in our system. Thermoelastic dissipation, which is dominant in the high frequency measurements of ref. [1], is not an issue with the low frequency tuned springs studied here. The data used in this paper is taken from measurements of TAMA-SAS with MGAS filters [20, 11, 12], and the Advanced LIGO passive SAS prototypes equipped with GAS filters [21], while the hysteresis measurements were done on the setup described in figure 1. The TAMA-SAS MGAS filters use a three blade configuration similar to the springs of figure 1. They do not have analog frequency tuning devices, but are pre-designed and machined to achieve a target working frequency, therefore they are not well suited to explore the spring behavior for different frequencies. The setup of figure 1 is particularly suitable for easily changing the resonant frequency and exploring the low frequency behavior of the MGAS springs.

The hysteresis effect has been observed in all springs and flex joints, made with similar precipitation hardened materials. This effect is simply progressively more visible in “softened”, low resonant frequency oscillators because of their smaller restoring force. This new understanding of damping and hysteresis behavior may allow tuning of MGAS filters and IPs to even lower frequencies. Lower frequency tuning of mechanical oscillators may be a key factor in providing passive seismic attenuation over a wider frequency band for future, advanced, low frequency GW interferometers.

The observed effects for Q-factor

Figure 2 indicates that the quality factor of the IP decreases with decreasing natural frequency [22, 21]. This behavior is compatible with a minimum intrinsic Maraging Q-factor of ~one thousand. Figure 3 and figure 4 illustrate the dramatic effect on Q when tuning the IP and the MGASF to a lower frequency respectively. For load closer to the critical load [23], the load at which critical damping is achieved, the IP becomes critically damped and hysteresis is observed. Similar Q-factor (figure 5) and hysteresis behaviors were measured in MGAS filters at frequencies one order of magnitude higher [7, 11] than the IP.

Observed hysteresis

Hysteresis was observed in all afore mentioned oscillators. Most of the measurements reported below were performed on the two blade MGAS spring, shown in figure 1. In this setup the vertical oscillation frequency was tuned by changing the radial compression by means of screws. Each time the blade’s base clamp position was released, tuned, and re-bolted tightly to the support plate. A vertical ruler resting on the base plate was used to measure the height of the equilibrium point. A stopwatch was used to measure the period of oscillation (typically over 5 oscillations). The cantilever blade, whose profile is also shown in figure 1, was 2x365 mm long, 35 mm wide at the base and 1.5 mm thick. The blades are flat at construction and bend under load to an almost uniform radius of curvature.

A continuum of equilibrium points can be obtained in a MGAS spring tuned to low frequency by slowly forcing excursions of large amplitude (and direction) and then slowly and monotonically reducing the applied force until the oscillator reaches the new equilibrium point. A larger range of equilibrium points is achieved by tuning the springs to lower resonant frequency. Note that, once a metastable equilibrium point is reached, small oscillations do not alter it and the oscillator behaves normally around it. This effect was used for generating the data shown in figure 6. This measurement was repeated for two different payloads to illustrate how, for small oscillations, metastable equilibrium points that have the same frequency are equivalent, independent of how the equilibrium is reached. Progressively larger oscillations produce a steady drift towards a true equilibrium point. This effect is illustrated in figure 7.

The metastable positions exist around a “true” equilibrium point. If left undisturbed they are stable in time, but sufficiently large oscillations (typically larger than the distance between the metastable equilibrium point to the true equilibrium point) lead to the true oscillation equilibrium point. As already noted, small oscillations do not change the metastable equilibrium point while intermediate amplitude oscillations produce progressive drifts towards the true equilibrium point.

Note also that very few oscillations are necessary to dissipate the hysteresis and to return to the true underlying equilibrium point. For example the true equilibrium points in figure 7 were achieved with a quality factor as low as 2. The true equilibrium point is not recovered if the spring is tuned to such a low frequency that it is too close to critical damping. In this case there are no oscillations to dissipate the hysteresis and return the oscillator to its true equilibrium point. The oscillator then seems to act unpredictably and stops at seemingly random positions near the true equilibrium point. Due to this unpredictable behavior, MGAS and IP in real operating conditions have rarely been tuned much below Q-factors of 2, as they were erroneously assumed to be unstable below this value.

The fact that experimenters were not able to tune IPs and MGAS filters at lower frequencies effectively introduced an unnecessary limit to the low frequency attenuation performance of passive seismic attenuation systems.

The new understanding presented in this paper may help remove this limit.

Explanation of the observed damping and hysteresis effects

Initially we attributed the observed strong damping and hysteresis in MGAS springs to the insufficient clamping of the bases of the blades (in the monolithic MGAS it is the only connection point where slippage and stiction may happen). This hypothesis was unconvincing due to the fact that similar damping behaviors were observed with different clamping techniques (bolted or wedged clamps) and strengths. We finally rejected it after observing the reversibility of the hysteresis. After loading and clamping, normal oscillations only slightly change the amplitude of the stresses in the clamp and never change their sign. In these conditions any slippage in the clamp would produce a monotonic droop of the payload, an irreversible effect. The total absence of irreversible drifts proves that the origin of the hysteresis problem is not in the clamps, but rather in the blade material itself.

The absence of irreversibility and the stability of the metastable equilibrium points also rule out creep effects that, since the overall stress never changes sign, would also produce unidirectional effects.

It is important to mention that the metastable equilibrium positions, far from the true equilibrium point (6 mm for this test, both above and below the true equilibrium point) have been observed to be stable within the measurement errors (0.25 mm) over the time scale of weeks. Therefore, we conclude that there is no significant creep (processes triggered by atomic level thermal fluctuations) associated with the metastable equilibrium points.

After elimination of these two hypotheses, detailed understandings of the observed effects required an understanding of:

- a) the microscopic behavior of precipitation hardened materials used in suspension springs and,
- b) its coupling to the macroscopic behavior of the blades.

The first seismic attenuation filter springs in the Virgo super-attenuators were made with ordinary spring steel and exhibited large, unacceptable, creep, i.e. drooping of the equilibrium position of tens of microns per day [24].

The solution to the creep problem was found with the use of precipitation hardened materials like Maraging steel or Copper Beryllium bronze. The (oversimplified) microscopic mechanism that eliminates the creep is discussed as follows.

When a spring of normal material (carbon steel for example) is stressed, the stress initially distributes equally throughout the volume of each grain. The dislocations present in each grain, started by atomic scale thermal fluctuations and pushed by the stress field, progressively drift towards the edge of the grains. Drifting dislocations drag stress along and thus concentrate it on the edges of each grain. Eventually, the stress buildup is sufficient to locally overcome the material's yield point, a grain fails by releasing part of its stress and emits acoustic energy.

Creep is common in most ordinary springs, but its effect is so small in absence of anti-springs that it is rarely noticed, and is often irrelevant in the normal lifetime of a spring. The high stability requirements of GWID's seismic attenuation systems, and the amplified drift due to the artificially engineered softness of the springs, made this problem visible and intolerable.

The solution for the creep problem is to block the movement of the dislocations that drive it. In precipitation hardened materials this is achieved by generating intermetallic precipitates interspersed inside each of the material's grain.

Maraging, commonly used in GWID seismic isolation systems, is an Iron alloy containing a large percentage of Nickel, Cobalt and other metals[†]. In molten phase,

[†] Maraging steel is a precipitation hardened alloy. The springs used in this study, and in most existing seismic attenuation systems are Marval 18 (also known as Marval 250), a trademark of Aubert Duval SA, 41, Rue de Villiers, Neuilly-sur-Seine, F-92202, France.

The composition is

Component	Percentage	Component	Percentage
C	≤ 0.03	Co	8.00
Fe	≥ 68.47	Mo	5.00
Ni	18.00	Ti	0.50

Cobalt, Nickel, Titanium, and the other solutes in the Iron solvent form a thermodynamically stable solution. The melt solidifies as an Austenitic material; a thermodynamically stable solid solution is obtained with no segregation of components. Cooling to room temperature causes the Austenitic crystals to flip into Martensitic ones. The solutes in the Martensitic crystals now form a metastable solid solution which, if the atoms were allowed to move, would segregate by forming precipitates. In practice though, all atoms are frozen in random locations of the lattice and they cannot segregate [25, 1].

Formation of precipitates is obtained by taking advantage of two properties of Maraging steel [26]. Firstly, while in maraging steel the transition from Austenite to Martensite happens below 100 centigrade (and is fully completed before reaching room temperature), the reverse process (from Martensite to Austenite) only happens above 600 degrees centigrade. Consequently, the Martensite with its supersaturated solid solution is stable over a wide range of temperatures. Secondly, above 400 centigrade the probability of two atoms interchanging position in the Martensite crystal becomes non negligible, and the atoms in solution effectively start a random walk within the Martensite structure. They occasionally interact with each other to form stable precipitates. The precipitates,[‡] originated from position exchanges between individual atoms, do not disrupt the continuity of the surrounding Martensite grain, they having different elastic properties than the rest of the grain material, provide point-like discontinuities. The diffusion and precipitation process happens on the timescale of hours (a few to hundreds, depending on the ageing temperature) and in a spatial scale of nanometers. Typical distances between precipitates are 10 to 30 nm [27, 28] (with smaller separation obtained with longer precipitation at lower temperature) to be compared with a typical grain size of 10 to 20 microns. Billions of precipitates form in each grain.

The interesting metallurgical property of these precipitates is that they impede the movement of the dislocations that are at the base of the creep processes. The dislocations actually move quite freely between precipitates in the relatively soft Iron lattice, even more freely than in the original un-precipitated solution, but they cannot drift across the precipitates and therefore, their movement stops within a few nanometers. Having stopped the long range movements of the dislocations, the stress does not concentrate anymore on the grain periphery and, after a short period of a few hours in which dislocations lean to the nearest precipitate, creep and acoustic emission stop altogether. Indeed creep was observed to stop below the upper limit of one grain failure per day per filter even with stresses close to the material's yield point [29, 30, 31]. Following these observations, Maraging was almost universally adopted as the material of choice for GWID suspensions.

The hardening process also greatly increases the intrinsic Q factor of Maraging, reflecting the fact that dislocations, now much less free to drift under the varying stress fields, cannot sap much energy from the oscillatory motions.

The residual losses are compatible with the fact that some dislocations are actually free to slush, although for exceedingly small distances, between precipitates. This effect explains the observed high, but not exceptional Q-factor of this material [1].

[‡] Typically Fe₂Mo, Ni₃Mo, Ni₃Ti nano-crystals

It is observed that MGAS springs, although built with the same materials as IPs, present a Q-factor that vanishes at frequencies more than one order of magnitude (two orders of magnitude in stiffness) higher than IPs.

This observed discrepancy can be understood as follows.

MGAS springs can be modeled as a set of normal springs (fishing rod movement of the cantilever blades) coupled to an antispring (the vertical projection of the radial compression of opposite blades). In MGAS springs, elastic oscillation energy flows between the cantilever spring (which tends to uniformly bend the entire blade) and the antispring (the radial compression which tends to increase the bend of the central portion of the blades while distending the rest). In other terms the region of maximum bending of a MGAS spring, moves back and forth along the blade's length during the oscillation, thus involving a relocation of the static stress over a large fraction of the MGAS blade. Conversely, in an IP oscillation, the stress of the flex joint simply increases and decreases by a very small fractional amount within a small stationary location.

Since the dissipated energy is proportional to the total elastic energy transfers (or, if one prefers, the loss is proportional to the amount of available dislocations that slosh around) much more losses can be expected in MGAS springs than in IPs. A quantitative answer can probably be obtained with a detailed comparative study of the MGAS and IP behaviors using a finite element analysis. This analysis, though, is quite time consuming. Therefore, the above qualitative comprehension of the discrepancy, along with the measurement of the actual losses in MGAS springs and IPs, are deemed sufficient for now.

How to explain the hysteresis?

Hysteresis becomes apparent both in IP and MGAS springs when the oscillation Q-factor gets close to unity. The transition from critically damped to hysteretic is quite similar in both systems, but at frequencies again differing by one order of magnitude.

The intermetallic precipitates are usually thought of as roadblocks that simply stop the dislocations without locking them in place [28]. In this idealization dislocations would generate damping, but not hysteresis. While the precipitates are almost ideal dislocation roadblocks, they are not quite perfect. If weak adhesion between precipitates and some dislocations is present, some fraction of the dislocations will not be completely free to slosh and may stick to the precipitate against which they come to a rest until a sufficiently strong counter stress frees them again. Since dislocations carry stress, sticking dislocations act like sticking applied stress, and this would definitely cause hysteresis. The application of increasing stress, like for example pushing the spring far from its equilibrium point, induces the movement of a growing number of dislocations, of which the fraction that sticks provide the memory process necessary to induce the observed hysteresis.

To produce the observed reversibility of the hysteresis phenomenon, the stickiness of the dislocations to the precipitates has to be such that the dislocations can be shaken loose by simply reversing the direction of the stress to a value comparable but somewhat smaller than the one that generated the hysteresis in the first place.

In the IP case the resonant frequency is typically tuned down from 3-4 Hz (unloaded leg) to less than 20mHz before the Q factor gets close to unity and the hysteresis becomes

observable. Tuning to low frequency with gravitational anti springs, lowers the IP's apparent stiffness by more than 4 orders of magnitude while the actual flex joint stiffness remains unaffected. This fact means that only 10^{-4} of the elastic energy needs to be transferred to sloshing dislocations (and get dissipated) to explain the observed Q-factors. It is sufficient to postulate that 10% or less of the sloshing dislocations that account for the damping effect get temporarily tangled to a precipitate in order to account for the observed hysteresis slope in figure 7.

Why then should MGAS springs also show hysteresis at 10 times higher frequency than IPs? The argument is essentially the same that explained the higher observed damping. The oscillation of a low frequency MGAS filter causes a lot of elastic energy to glide back and forth over macroscopic distances along the spring's length, while in IP the stress is stationary and the static stress only change intensity by relatively small amounts. The stress field that in an oscillating MGAS glides along the blade actually corresponds to the entire static stress field that supports the payload against gravity. The stress movements along the blade's length are comparable with the oscillation amplitude. The variations of elastic energies in play in MGAS are much larger than in IP flex joints and so the same sticking fraction of dislocations can explain the stronger effect. It is therefore not surprising that, similar to damping, much larger hysteresis is observed at much higher frequencies in MGAS than in IPs.

We observed that Copper Beryllium MGAS springs achieved the $Q \sim 1$ regime and hysteresis faster than as similar Maraging MGAS. This observation indicates that Copper Beryllium intermetallic precipitates may be less effective in immobilizing dislocations and/or stickier than the Maraging ones.

How to take advantage of the new understanding?

Lowering the resonant frequency of an oscillator shifts the pole of the filter transfer function to lower frequency and provides larger attenuation. Such an expanded attenuation capability in a gravitational wave interferometer would substantially reduce the low frequency integrated r.m.s. motion of the mirror payload, i.e. drastically reducing the force requirements for the mirror suspension actuators and noise from the controls associated with them. Therefore it would be of great interest to operate passive filters at the lowest possible frequency, maybe even deep in the critically damped and strongly hysteretic regime.

Even in the very low frequency critically damped and hysteretic regime, the underlying true equilibrium point can be retrieved by forcing an oscillation (the same way the old watches were demagnetized by placing them in Helmholtz coils and subjecting them to oscillating magnetic fields of decreasing amplitude). The problem is that the MGAS tuning is done by allowing free oscillations while the experimenter changes the load and radial compression until the desired minimum oscillation frequency is obtained. This tuning is not possible using the traditional method if the spring is in the critically damped regime and is not capable of oscillating. We are experimenting with practical techniques to achieve this tuning. These solutions involve the use of temporary parallel tuning springs and/or electro-magnetic tunable auxiliary springs. We have already successfully tested low frequency tuning of MGAS with this technique [17] Care must be taken because at lower frequencies the oscillators are naturally more thermally

sensitive. A suitable method of thermally compensating the changing elastic modulus of the blade material must be implemented to avoid large thermal changes of the equilibrium point and to allow for reliable use of the springs, otherwise very low frequency springs would be relegated to well thermally stabilized environments. The same electro magnetic spring used for tuning, can provide the thermal correction mechanism. Ongoing work is addressing these issues.

Can we make low frequency oscillators with less damping and hysteresis?

Our observation suggests that, by identifying the proper material, hysteresis and damping can be strongly reduced. Following the idea, we are investigating materials suitable for use in MGAS blades close to the mirror final suspensions, and then we will compare their performance with that of Maraging and Copper Beryllium.

The idea is to use material without (instead of “with frozen”) dislocations. The obvious solution is glassy metals that, with no crystalline lattice, have no dislocations and have the added advantage that they allow almost twice the elongation as a normal metal before yielding. Therefore glassy metal blades could carry more payload using less blade material, which allows for even better attenuation performance.

A promising candidate for the purpose is Vitreloy 001, produced by Liquidmetals for golf clubs and other uses. Vitreloy 001 is also non magnetic, which is an advantage near the final mirror suspensions. We are presently attempting to produce of Vitreloy 001 blades for mirror suspensions testing.

Conclusions

A new understanding of anomalous damping and hysteresis in low frequency springs is presented. It may allow for passive attenuation at even a lower frequencies regime than achieved so far, thus further reducing the requirements on the mirror suspension control actuators and reduce their associated noise in GWID. Vertical filters tunable to lower frequency could be the solution to match the frequency performance of longer suspensions of lower frequency attenuation systems in future underground Gravitational Wave Detection Interferometers.

Acknowledgments

The LIGO Observatories were constructed by the California Institute of Technology and Massachusetts Institute of Technology with funding from the National Science Foundation under Cooperative Agreement PHY 9210038. The LIGO Laboratory operates under Cooperative Agreement PHY-0107417. This paper has been assigned LIGO Document Number LIGO-P030040-00-D.

References:

- [1] S. Braccini, et al., “The Maraging-Steel Blades of the Virgo Super Attenuator”, *Meas. Sci. Technol.* 11 (2000) 467- 476. And Erratum in *Meas. Science Technol.* (March 2004)
- [2] S. Braccini, et al., “The Maraging Steel Blades of the Virgo Super Attenuator”, *Proceedings of CP523, Gravitational Waves: Third Edoardo Amaldi Conference* (2000)
- [3] S. Braccini, et al., “Seismic Vibrations Mechanical Filters for the Gravitational Waves Detector VIRGO”, *Rev. Sci. Instrum.*, 67 (1996), 2899-2902
- [4] V. Sannibale, et al., “Monolithic Geometric Anti-Spring blades”, LIGO-040004-00-D available at <http://admdbsrv.ligo.caltech.edu/dcc/>
- [5] Sz. Márka, et al., “Anatomy of the TAMA SAS Seismic Attenuation System”, *Proceedings of 2001 Amaldi Meeting, LIGO Report, LIGO-P-010034-00-D* available at <http://admdbsrv.ligo.caltech.edu/dcc/> (*Class. Quantum Grav.* 19 (2002) 1605-1614)
- [6] A. Bertolini, et al., “Seismic Noise Filters, Vertical Resonance Frequency Reduction with Geometric Anti-Springs: A Feasibility Study”, *Nucl. Instr. and Meth. A* 435 (1999), 475-483
- [7] V. Sannibale, et al., “Seismic Attenuation Performance of the First Prototype of a Geometric Anti-spring Filter”, *Nuclear Inst. and Methods in phys. Research A* 487 (2002) 652-660
- [8] M. V. Plissi, et al., "GEO 600 triple pendulum suspension system: Seismic isolation and control" *Rev. Sci. Instrum.* Vol 71(6) (2000), 2539-2545
- [9] B. Abbot, et al., “Detector Description and Performance for the First Coincidence Observations between LIGO and GEO”, LIGO-P-030024-00-R available at <http://admdbsrv.ligo.caltech.edu/dcc/>
- [10] “Advanced Ligo:Content and Overview”, Proposal to NSF, LIGO-M-030023-00-R available at <http://www.ligo.caltech.edu/docs/M/M030023-00/>
- [11] V. Sannibale, et al., “A New Seismic Attenuation Filter Stage (MGASF) For Advanced Gravitational Interferometer Detectors”, submitted to *Nucl. Instr. and Meth. A* (MGASF mechanical details are available at LIGO-D-010241-00-R)
- [12] V. Sannibale, G. Cella, et. al., “Monolithic GAS blades”, in preparation for submission to *Nucl. Instr. and Meth. A* (GASF mechanical details are available at LIGO-D-010242-00-R) get the real number and pub.
- [13] Winterflood, J., Barber T et al. “Using Euler Buckling Springs for Vibration Isolation.” *Class. Quantum Grav.* 19 (2002) 1639-1645

- [14] Personal communication, G. Losurdo
- [15] J. E. Ugas, et al., “Hysteresis Report of the Tama-SAS filters”, LIGO Report (2001), LIGO-T010036-00-R available at <http://admdbsrv.ligo.caltech.edu/dcc/>
- [16] Personal communication Aso
- [17] M. Mantovani, Master’s thesis, Universita’ di Pisa, work in progress.
- [18] A. Bertolini, et al., “Recent Progress on the R&D Program of the Seismic Attenuation System (SAS) Proposed For the Advanced Gravitational Wave Detector, LIGO II”, Nucl. Instr. and Meth. A 461 (2001), 300-303
- [19] Takamori, et al., “Seismic Attenuation System (SAS) Prototype Test”, available at <http://www.ligo.caltech.edu/docs/G/G030018-00/G030018-00.pdf>
- [20] A. Takamori, “Low Frequency Seismic Isolation for Gravitational Wave Detectors”, PhD Thesis, LIGO-P-030049-00-R available at <http://admdbsrv.ligo.caltech.edu/dcc/>
- [21] M. Ando, et al., “Report to NSF on the TAMA-SAS Passive Seismic Attenuation Chain Test for the Tokyo University 3 meter Interferometer”, LIGO-T-010006-00-R available at <http://admdbsrv.ligo.caltech.edu/dcc/>
- [22] Sz. Márka, et al., “Inverted Pendulum as Low Frequency Pre-Isolation for Advanced Gravitational Wave Detectors”, in preparation for submission to Nucl. Instr. and Meth. A (IP mechanical details available at LIGO-D-010240-00-R)
- [23] Sz. Marka, "Characterization of LIGO II/SAS Inverted Pendulum as Low Frequency Pre-Isolation, presented at APS April 2000 at Long Beach, California
- [24] R. DeSalvo, “Non Stochastic Noise in Gravitational Wave Detectors”, Proceedings of Second Edoardo Amaldi Conference on Gravitational Waves
- [25] K. Rohbach and M. Schmidt 1990 *Metals Handbook* 10th edn, vol 1 (Materials Park, OH: ASM) pp 793-800
- [26] V. K. Vasudevan et al., “Precipitation reaction and strengthening behavior in 18 wt pct nickel maraging steel” Metall. Trans. A 21 (1990) 2655–68
- [27] U. K. Viswanathan et al. “Precipitation hardening in 350 grade maraging steel” Metall. Trans. A 24 (1993) 2429–42
- [28] G. Saul et al., *Source Book on Maraging Steels*, American Society for Metals, 1979

- [29] A. Bertolini, et al., “The GAS Blade Creep Measurements, Problems and Some Solutions”, LIGO Report, LIGO-T-10112-00-R available at <http://admdbsrv.ligo.caltech.edu/dcc/>
- [30] R. Stellacci, et al., “Measurement of Metal Creep in Gravitational Wave Detectors”, LIGO Report (2001), LIGO-T010155-00-D available at <http://admdbsrv.ligo.caltech.edu/dcc/>
- [31] R. DeSalvo, et al., “TOTEM, Blade’s Creep Measuring Facility, Mechanical drawings LIGO drawings” (2001), LIGO-D-010252-00-R available at <http://admdbsrv.ligo.caltech.edu/dcc/>
- [32] G. Ballardini, et al., “Measurement of the VIRGO Supertenuator Performance for Seismic Noise Suppression”, Rev. Sci. Instrum. 72 (2001) 3643-3652
- [33] H. Tariq, et al., “The Linear Variable Differential Transformer (LVDT) position sensor for Gravitational Wave Interferometer low-frequency controls”, Nuclear Inst. and Methods in phys. Research A 489 (2002) 570-576
- [34] C. Wang, et al., “Constant Force Actuator for Gravitational Wave Detector’s Seismic Attenuation Systems (SAS)”, Nuclear Inst. and Methods in phys. Research A 489 (2002) 563-569
- [35] R. DeSalvo, et al., “TAMA Seismic Attenuation System (SAS) Tower”, LIGO Mechanical drawings (2001), LIGO-D- 010249-00-R, in: LIGO-II seismic attenuation system (SAS) test tower Filter-0, LIGO Mechanical drawings, LIGO-D-010241-00-R available at <http://admdbsrv.ligo.caltech.edu/dcc/>
- [36] A. S. Norwick et al., *Anelastic Relaxation in Crystalline Solids* (New York: Academic), 1972

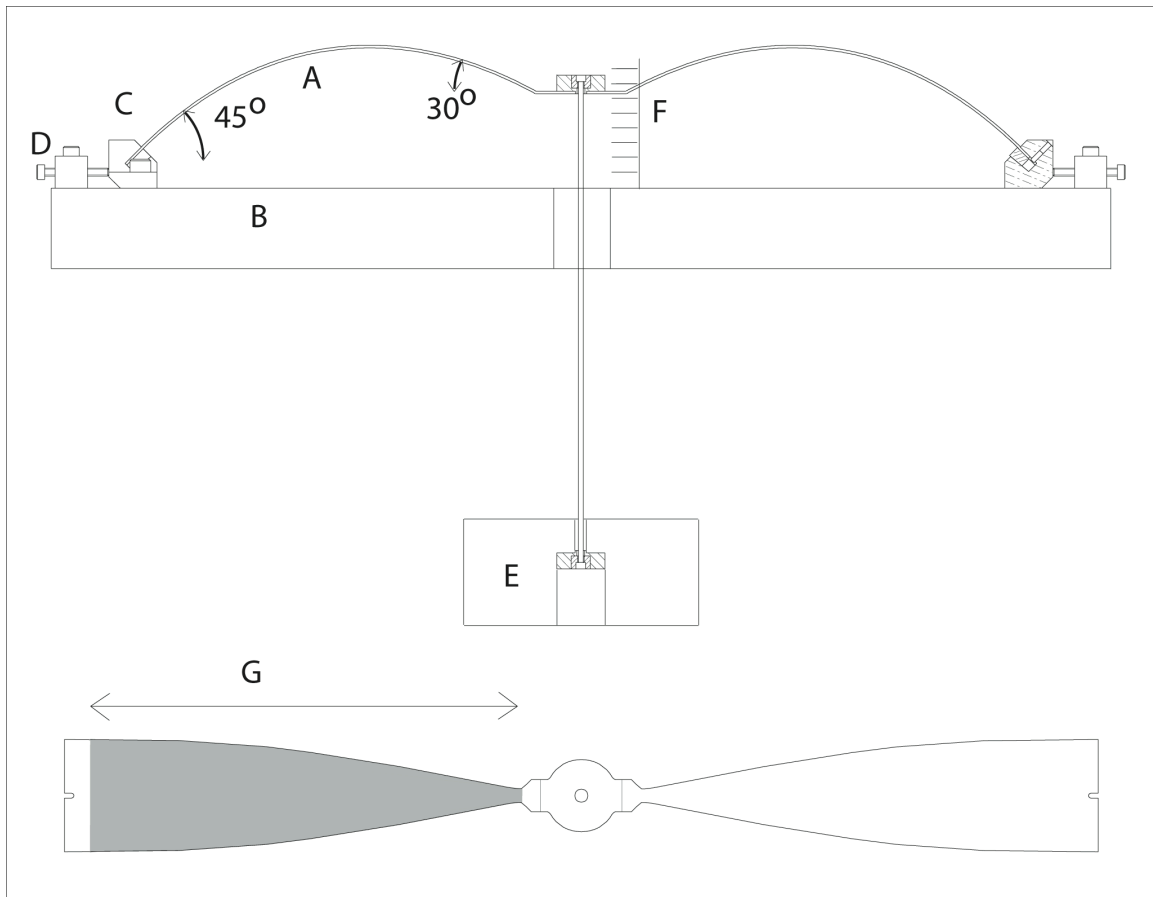


Figure 1: Twin blade MGAS spring used for the hysteresis measurement in this paper: A: blade, B: support structure, C: sliding blade clamp, D: frequency tuning set screws, E: Payload, F: position readout ruler, G: flexing portion of blade, the ogival profile of the blade is calculated to achieve a blade with nearly constant bending radius (uniform stress) at the working point.

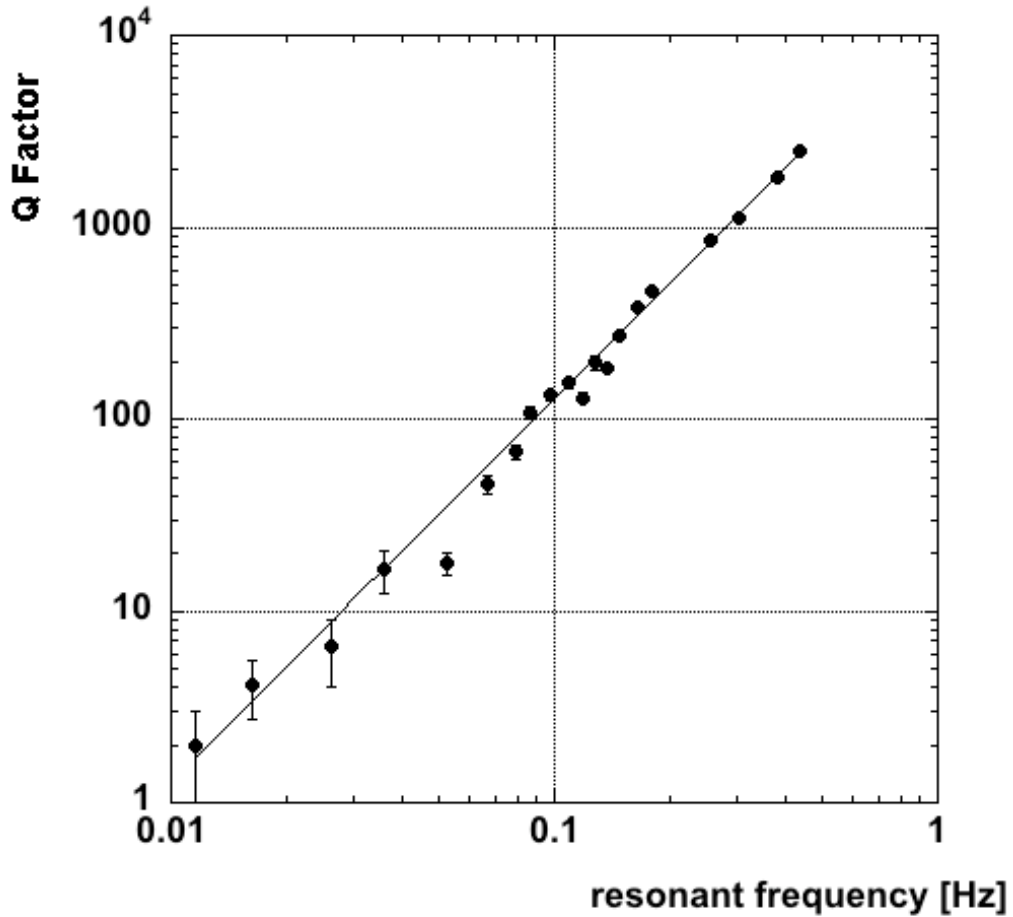
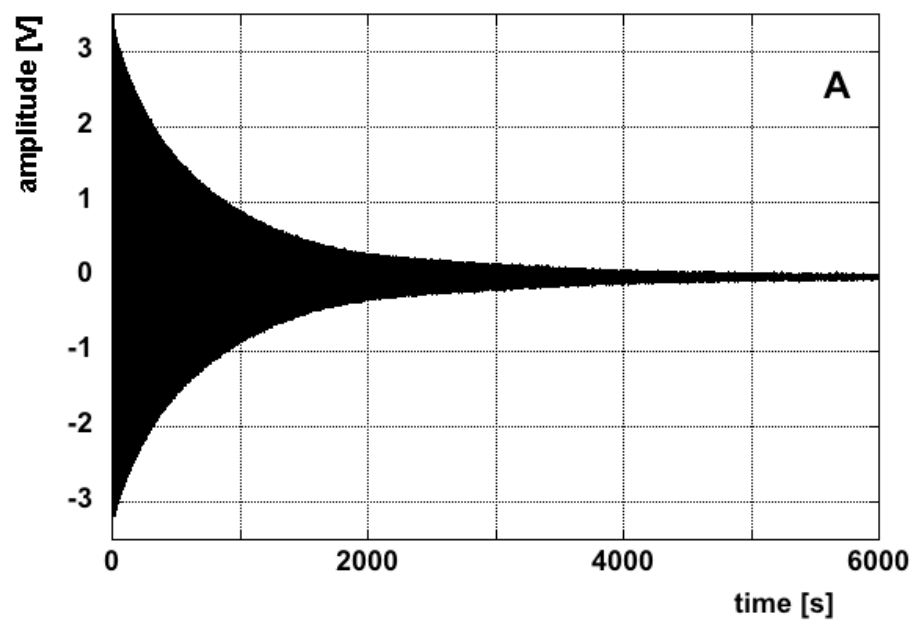


Figure 2: The Q factor of the IP versus its natural frequency. The relationship between is described approximately by a second order polynomial of the frequency; $Q = \left(\frac{1}{p}\right)\left(\frac{L}{g}\right)\omega^2$, where $L \sim 3$ m, $g \sim 10$ m/s². At 13 mHz the IP is essentially critically damped. The fit suggest that the loss factor, ϕ , is of order $\sim 10^{-3}$.



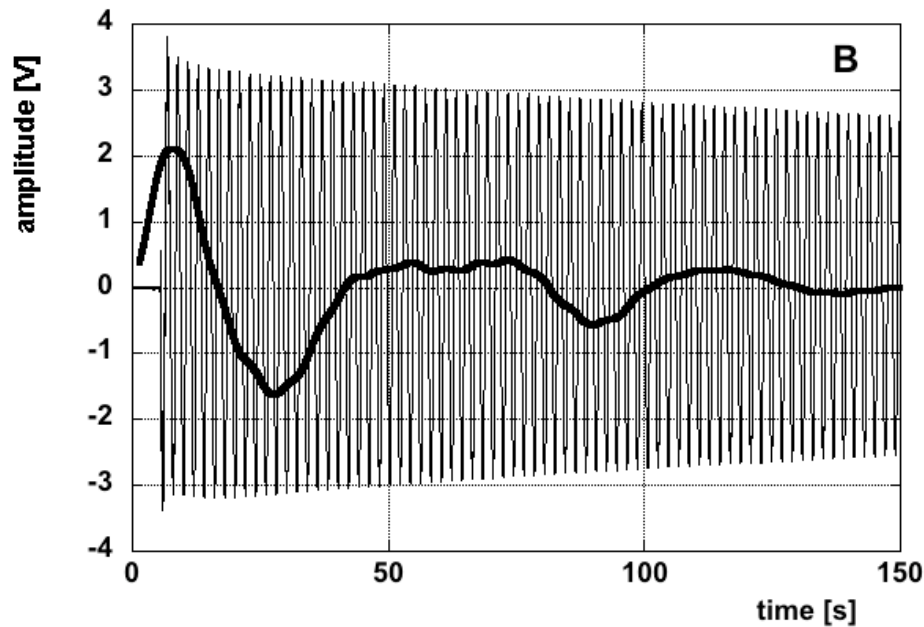
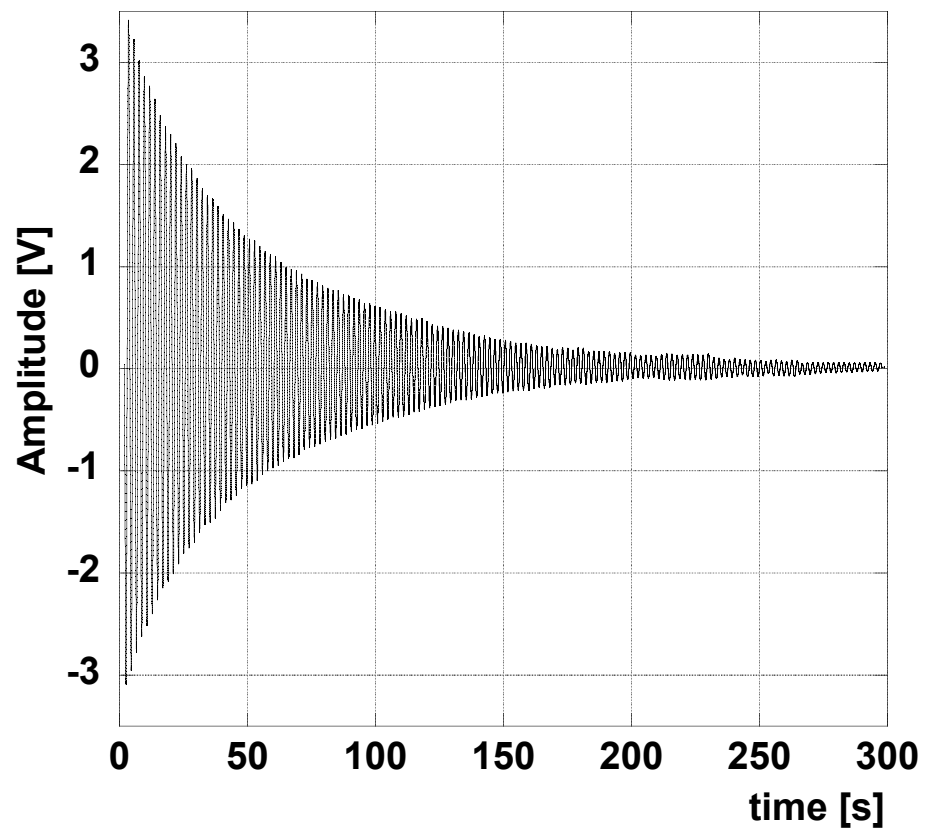


Figure 3: IP ringdown at low load (both graph A and, enlarged graph B) with a superimposed plot close to the critical load (thick line in graph B). The signal close to critical load shows irregularities due to several factors, including the interaction with the orthogonal oscillation degree of freedom, interactions with the air surrounding the IP and seismic excitations. Note the faster oscillation in the first period. This behavior is characteristic of large amplitude (\sim cm) oscillations for both GAS and MGAS springs. The IP has its minimal resonant frequency only within a narrow displacement range and presents somewhat faster oscillation frequency for larger oscillations. The effect is only visible at low frequencies where the spring and the antispring components virtually cancel each other and higher order terms become non negligible.



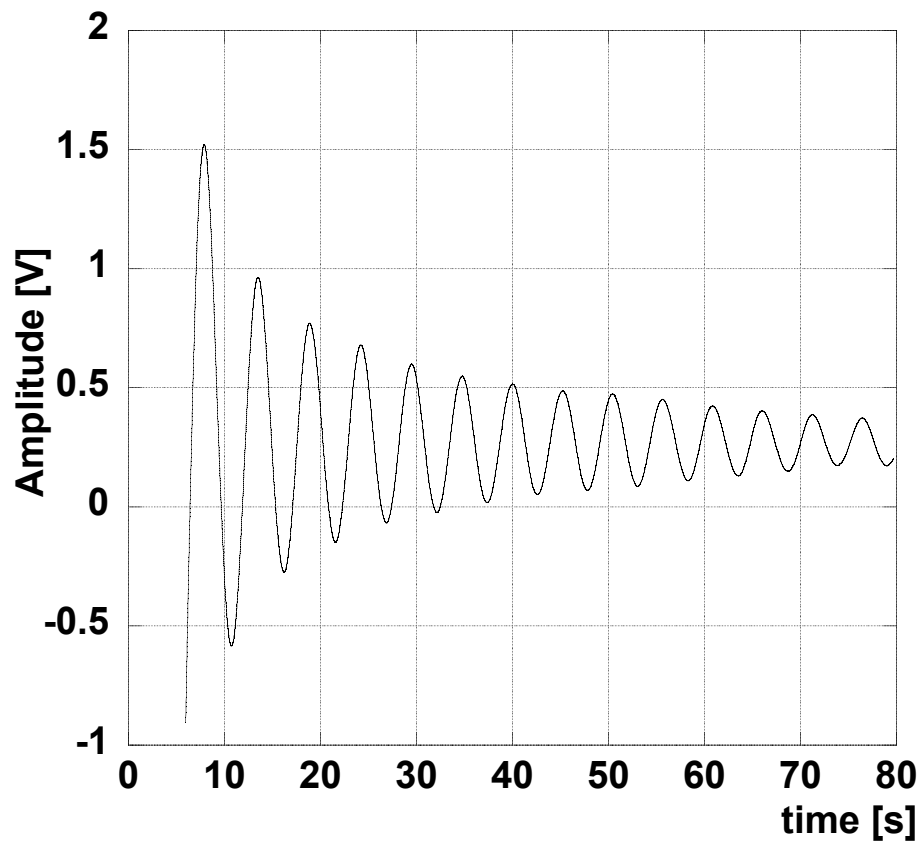


Figure 4: TAMA-SAS MGAS filter ringdown when larger radial compression factors produce smaller resonant frequencies.

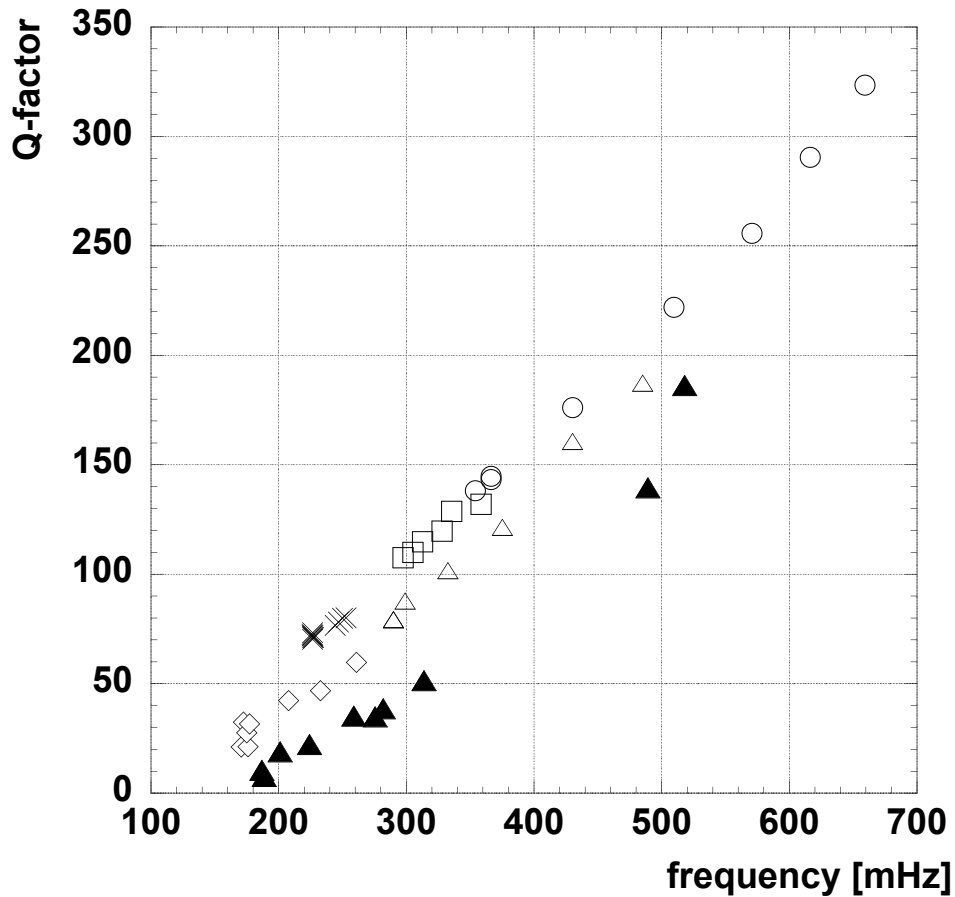


Figure 5: GAS (empty symbols) and MGAS (black triangles) filter Q factor versus frequency plot.

Unlike in the IP case, no good agreement is found with quadratic fit. The geometric anti springs have larger higher order terms in the elastic potential energy and do not obey the simple quadratic formula valid for the IP.

The different frequencies in the plot are obtained by simply changing the filter load (and equilibrium points) and performing the Q factor measurements for small oscillations around each equilibrium point. Note that the filters are not built for frequency tuning, they are machined for a target minimal frequency and need to be modified and re-assembled for different target frequencies. Therefore the oscillations presented in this set of measurements, obtained from the available filters which were machined for higher values of target minimal frequency, do not contain very low frequency data.

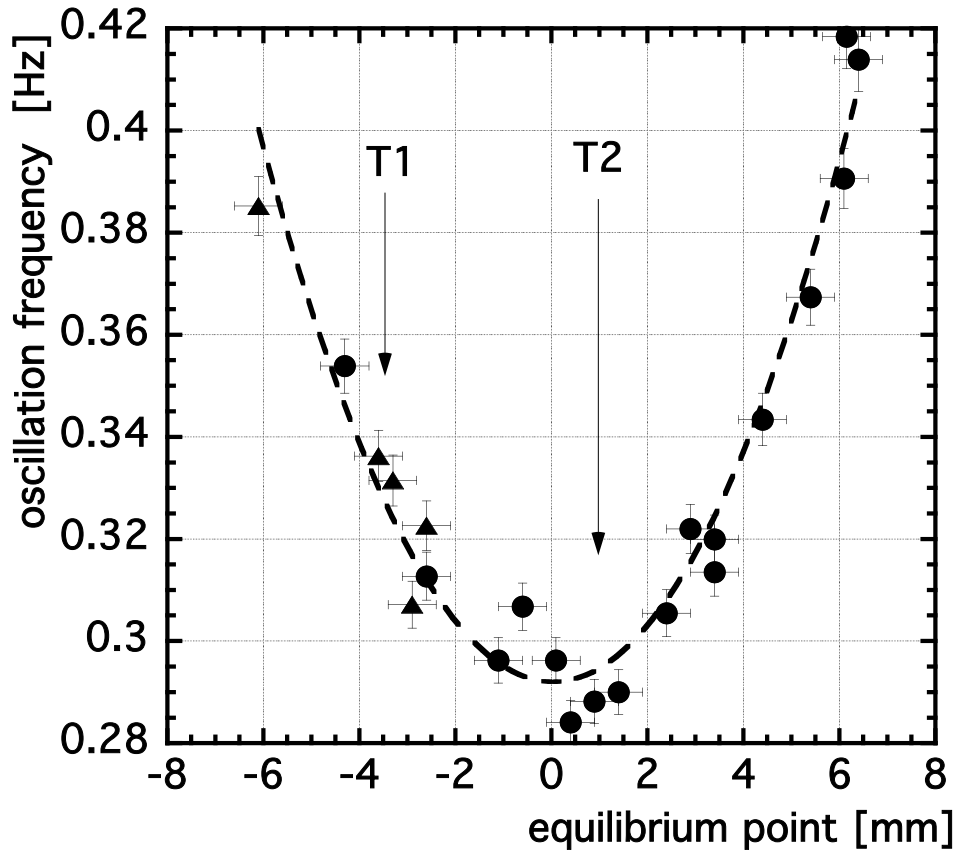


Figure 6: Oscillation frequency for small amplitudes versus equilibrium point of the MGAS. The difficulty in measurement arises from the fact that small oscillations are required not to significantly change the metastable equilibrium point. Small oscillation amplitudes, coupled to the low Q -factor (2 or less at these low frequencies) made the measurement difficult and the frequency error large. To produce the data for this figure, several metastable positions were achieved, as described in figure 7, around 2 different true equilibrium positions (T1 for the points labeled with triangles and T2 for the circles) corresponding to two slightly different payload values. The oscillation frequency and Q -factor only depend on the equilibrium point, regardless if it is a true or a metastable one. The horizontal error bar of 0.5 mm corresponds to the reading error of the ruler used to measure the equilibrium point height. The 1.5% vertical error bar derives from the experimenter and stopwatch precision (0.25s) over the duration of 5 oscillations (~ 15 s).

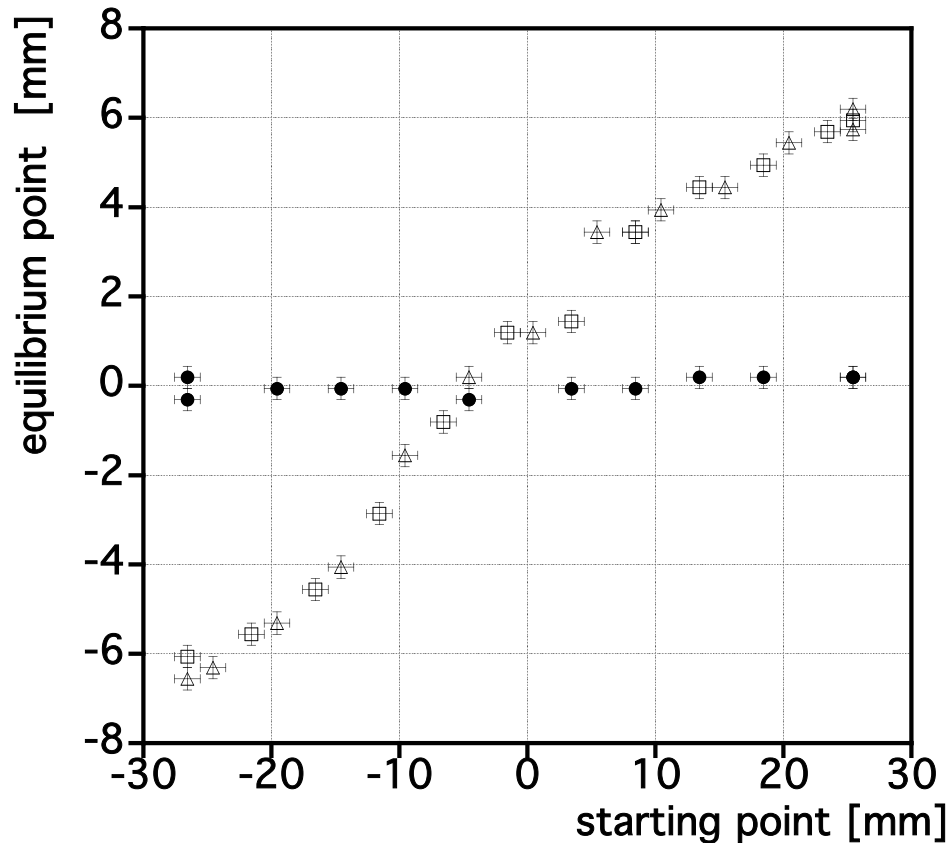


Figure 7: Equilibrium position reachable from different starting conditions. The triangles and squares correspond to the achievable metastable equilibrium points when the MGAS is manually forced to a given excursion (starting point on horizontal axis) and then the force is slowly reduced to zero until the corresponding metastable equilibrium point is reached without oscillations. The triangles and squares correspond to metastable positions reached from a previous metastable position above or below the true equilibrium point. The true equilibrium position (dots) is reached if the oscillator is forced to a given excursion and then left to freely oscillate. The error bars of 0.25 mm (0.5 mm on the starting point) correspond to the readout error of the ruler.